Cellular Signalling 54 (2019) 10–16

Contents lists available at ScienceDirect

Cellular Signalling

journal homepage: www.elsevier.com/locate/cellsig

Regulation of the stability and activity of CDC25A and CDC25B by protein phosphatase PP2A and 14-3-3 binding

Yuri Kohama, Megumi Saito, Mizue Yada, Hiroshi Sakurai*

Division of Health Sciences, Graduate School of Medical Science, Kanazawa University, 5-11-80 Kodatsuno, Kanazawa, Ishikawa 920-0942, Japan

ARTICLE INFO

Keywords:
CDC25B
14-3-3
PP2A
IER5
Dephosphorylation
Protein degradation

ABSTRACT

Cyclin-dependent kinase (CDK)-activating phosphatases, CDC25A and CDC25B, are labile proteins, and their levels vary in a cell cycle-dependent manner. Immediate-early response IER5 protein negatively regulates the cellular CDC25B levels, and stress-induced IER5 expression potentiates G2/M arrest. IER5 binds to protein phosphatase PP2A and regulates the PP2A substrate specificity. We show that IER5 binds to CDC25B and assists PP2A to convert CDC25B to hypophosphorylated forms. Hypophosphorylation at Ser323 results in the dissociation of CDC25B from 14-3-3 phospho-binding proteins. In IER5 expressing cells, CDC25B dissociated from 14-3-3 is unstable but slightly activated, because 14-3-3 inhibits CDC25B polyubiquitination and CDC25B binding to CDK1. The 14-3-3 binding to CDC25A also impedes CDC25A degradation and CDC25A-CDK2 interaction. We propose that 14-3-3 is an important regulator of CDC25A and CDC25B and that PP2A/IER5 controls the stability and activity of CDC25B through regulating the interaction of CDC25B and 14-3-3.

1. Introduction

Cyclin-dependent kinases (CDKs) and the regulatory subunits Cyclins are essential players in cell-cycle progression. Dual-specificity phosphatase CDC25 activates the CDK/Cyclin complex by dephosphorylating inhibitory phosphorylation at threonine 14 (Thr14) and Tyr15 on CDK. There are three CDC25 isoforms, CDC25A, CDC25B, and CDC25C. CDC25B and CDC25C play a predominant role in the G2-M transition by regulating the activity of CDK1/Cyclin B, whereas CDC25A is mainly implicated in the G1-S transition through CDK2/Cyclin A regulation but also has a role in the G2-M transition [1–3]. CDC25 phosphatases are labile proteins, and CDC25A and CDC25B levels vary in a cell cycle-dependent manner. Checkpoint pathways are activated in response to genotoxic stress and mediate the degradation or inactivation of CDC25. CDC25 overexpression has been reported in various cancers, associating with poor prognosis. Phosphorylation is the major post-translational modification of CDC25, changing activity, stability, and cellular localization [1–4].

Phospho-binding family proteins 14-3-3 consist of seven isoforms (β, ε, γ, η, σ, τ/θ, and ζ). 14-3-3 proteins integrate and regulate multiple signaling pathways. The effects of 14-3-3 binding to the phosphorylated proteins vary depending on the protein: stabilization or destabilization, activation or inactivation of the activity, regulation of subcellular localization, and linking two proteins as an adaptor [5–7]. CDC25 phosphatases are clients of 14-3-3. The interaction with 14-3-3 is required for cytoplasmic localization of CDC25B and CDC25C [8–11]. This also blocks access to the substrate CDK/Cyclin and inhibits the activity of CDC25A and CDC25B [9,12–15]. Under DNA damage conditions, 14-3-3γ functions as a platform for generation of complexes between CDC25A and CHK1, which results in phosphorylation and degradation of CDC25A [16].

Expression of CDC25B is negatively regulated by immediate-early response IER5 protein [17,18]. IER5 is a potential transcription factor and inhibits *CDC25B* gene expression through binding to the promoter [17]. IER5 participates in the regulation of cell proliferation under normal physiological and stressed conditions [17,19–22]. IER5 is a 327-amino acid protein and its N-terminal region, which shares homology to other IER proteins, IER2 and IER5L, binds to B55 family regulatory subunits (B55α, B55β, B55γ, and B55δ) of protein phosphatase 2A (PP2A) [23]. PP2A, the most abundant serine/threonine phosphatase, plays an important role in various cellular processes, especially in cell-cycle progression [3,24,25]. IER5 also interacts with PP2A target proteins, including heat shock factor 1 and ribosomal protein S6 kinase, and enhances PP2A activity toward these proteins [21–23].

In this report, we show that IER5 negatively regulates the stability of CDC25B. IER5 binds to CDC25B and enhances CDC25B

* Corresponding author at: Division of Health Sciences, Graduate School of Medical Science, Kanazawa University, 5-11-80 Kodatsuno, Kanazawa, Ishikawa 920-0942, Japan.
E-mail address: hsakurai@staff.kanazawa-u.ac.jp (H. Sakurai).

https://doi.org/10.1016/j.cellsig.2018.11.017
Received 23 August 2018; Received in revised form 19 November 2018; Accepted 19 November 2018
Available online 20 November 2018

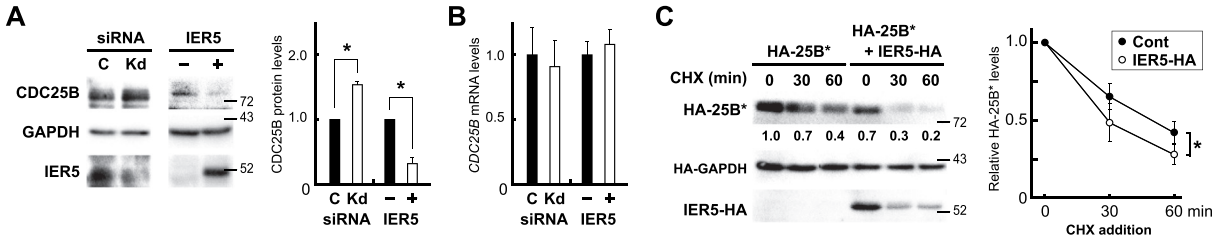

Fig. 1. Effects of IER5 on CDC25B protein levels.
(A) CDC25B protein levels in IER5-silenced and IER5 overexpressing cells. In left panels, HeLa cells were transfected with IER5 siRNA (Kd) or scrambled siRNA (C). In right panels, cells were transfected with pEBMulti-Hyg carrying IER5, and cells stably expressing IER5 were selected by hygromycin B. Cell extracts were subjected to western blotting. Positions of molecular mass markers are shown on the right. The relative CDC25B protein levels were determined after normalization to the GAPDH protein levels and expressed as the mean ± SE of three independent experiments (* $p < .05$).
(B) *CDC25B* mRNA levels in IER5-silenced and IER5 overexpressing cells. Cells were cultured as in (A). The relative *CDC25B* mRNA levels were determined after normalization to the *GAPDH* or *β-actin* mRNA levels and expressed as the mean ± SE of three independent experiments.
(C) Stability of CDC25B in IER5 expressing cells. HA-CDC25B* and HA-GAPDH expression constructs were transfected along with IER5-HA expression construct. Cells were treated with 40 μg/ml cycloheximide (CHX) for 0, 30, and 60 min, and extracts were subjected to western blotting. Numbers show the HA-CDC25B* levels determined after normalization to the HA-GAPDH levels with comparison to the initial levels of control cells. Relative levels of HA-CDC25B* with comparison to the initial levels were expressed as the mean ± SE of three independent experiments (* $p < .05$).

hypophosphorylation by PP2A, which leads to CDC25B dissociation from 14-3-3. 14-3-3 stabilizes CDC25B and inhibits its binding to CDK1. Similar effects of 14-3-3 are also observed for CDC25A. Our findings demonstrate that PP2A/IER5 plays an important role in the CDC25B and 14-3-3 interaction regulating the stability and activity of CDC25B.

2. Materials and methods

2.1. DNA constructs

The coding regions of CDC25A, CDC25B3, GAPDH, 14-3-3β, and 14-3-3ε were amplified by RT-PCR from HeLa total RNA and cloned into pcDNA3.1(+) (Invitrogen, Carlsbad, CA, USA). The tag sequences of HA, Myc, and FLAG were created at the N- and C-terminal regions [21,23]. CDC25A mutant (CDC25A*) exhibiting reduced binding ability to CDK1, CDK2, Cyclin B1, and Cyclin A contained R446L, R450L, and Y455A substitutions [26]. CDC25B mutant (CDC25B*) exhibiting reduced binding ability to CDK1 and Cyclin B1 contained a Y511A substitution [14]. Phosphatase defective mutants of CDC25A (CDC25A**) and CDC25B (CDC25B**) contained C430S and C487S substitutions, respectively [27]. 14-3-3ε mutant exhibiting reduced binding ability to its target proteins contained K50E and K118E substitutions [28]. The expression constructs of IER5, IER5 deletion derivatives, and B55 family members were described previously [21,23].

2.2. Cell culture and transfection

HeLa cells were cultured as described previously [21]. Transfection was conducted using Lipofectamine 3000 (Invitrogen) and RNAiMAX (Invitrogen) reagents. The following siRNAs were used: IER5, 5′-CCG GGAACGUGGCUAACCUTT-3′ and 5′-AGGUUAGCCACGUUCCCG GTT-3′; scramble, 5′-CCUACGCCACCAAUUUCGUTT-3′ and 5′-ACGAA AUUGGUGGCGUAGGTT-3′.

2.3. Quantitative PCR analysis

RNA isolation, cDNA synthesis, and real-time quantitative PCR were performed as described previously [29]. The following primers were used: *CDC25B*, 5′-ACTCTAAGGCCTTCCTCC-3′ and 5′-CACCGCAGTCT TGATGTG-3′; *GAPDH*, 5′-GTTCGACAGTCAGCCGCATC-3′ and 5′-GGA ATTTGCCATGGGTGGAA-3′; *β-actin*, 5′-ACTGGGACGACATGGAG AAA-3′ and 5′-GTCTCAAACATGATCTGGGT-3′.

2.4. Immunoprecipitation and western blot analysis

Cell extracts were subjected to SDS-polyacrylamide gel electrophoresis (PAGE) with/without Phos-tag (Wako Pure Chemicals, Osaka, Japan) and analyzed by western blotting as described previously [21,23,29]. For immunoprecipitation, cells were lysed in IP buffer (20 mM Tris-HCl, pH 7.6, 0.1 M NaCl, 0.5% NP-40, 0.5 mM phenylmethylsulfonyl fluoride, protease inhibitor cocktail (Nacalai Tesque, Kyoto, Japan), and phosphatase inhibitor cocktail (Nacalai Tesque)), and cleared cell extracts were incubated with an antibody and protein A Sepharose CL-4B (GE Healthcare, Buckinghamshire, UK) [21]. The antibodies used were anti-IER5 (AP17351c, Abgent, San Diego, CA, USA), anti-CDC25B (9525S, Cell Signaling Technology Japan, Tokyo, Japan), anti-phospho CDC25B (Ser323) (A0063, Assay Biotechnology, Sunnyvale, CA, USA), anti-CDC25A (sc-7389, Santa Cruz Biotechnology, Santa Cruz, CA, USA), anti-phospho CDC25A (Ser178) (E11-8017A, EnoGene Biotech, New York, NY, USA), anti-phospho CDC25A (Thr507) (AP3051a, Abgent), anti-CDK1 (ab133327, Abcam, Cambridge, MA, USA), anti-phospho CDK1 (Tyr15) (AF888, R&D Systems, Minneapolis, MN, USA), anti-CDK2 (ab32147, Abcam), anti-phospho CDK2 (Thr14) (ab68265, Abcam), anti-HA (M180, MBL, Nagoya, Japan), anti-Myc (M192, MBL), anti-FLAG (M185, MBL), and anti-GAPDH (G9545, Sigma-Aldrich, St Louis, MO, USA).

2.5. Statistical analysis

The data are representative of at least three independent experiments. Significant differences were determined by Student's *t*-test.

3. Results

3.1. CDC25B is rapidly degraded in IER5 expressing cells

To examine whether IER5 affects the expression of CDC25B, western blot analysis was conducted. The levels of CDC25B protein increased when IER5 was knocked down using siRNA (Fig. 1A). In contrast, IER5 overexpression resulted in a decrease in CDC25B. These changes were not due to the expression of *CDC25B* mRNA because the mRNA levels were not significantly affected by depletion or overexpression of IER5 (Fig. 1B). Rather IER5 affected the stability of CDC25B protein. A CDC25B mutant containing a Y511A substitution (CDC25B*) exhibits severely reduced binding ability to CDK1/Cyclin B1 and does not affect cell-cycle progression [14]. The levels of exogenously expressed HA-CDC25B* were rapidly reduced after addition of cycloheximide with a half-life of 45 ± 7 min (Fig. 1C). In IER5 expressing cells, CDC25B

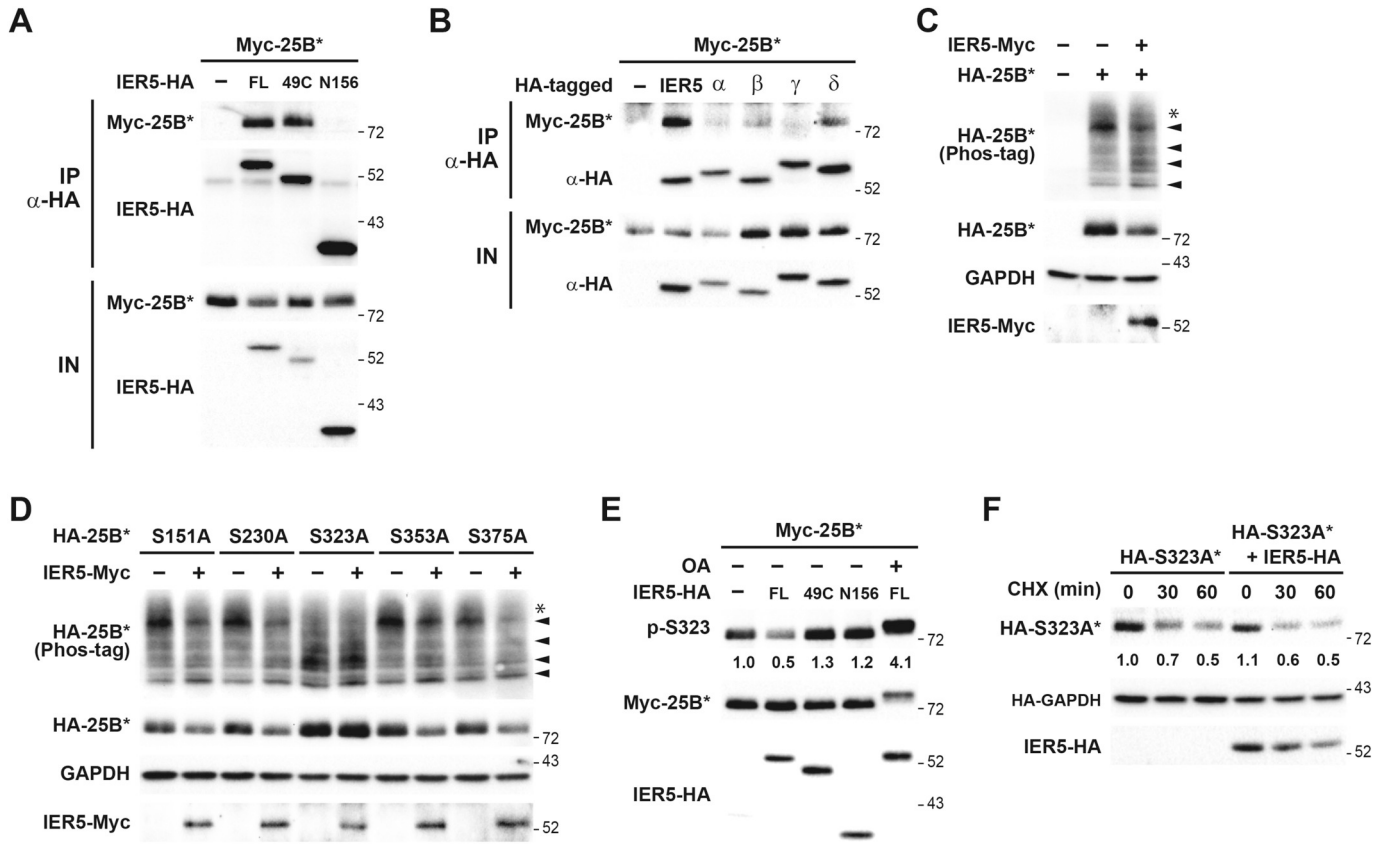

Fig. 2. Effects of IER5 on phosphorylation status of CDC25B.

(A) Co-immunoprecipitation analysis of IER5 derivatives with CDC25B. Myc-CDC25B* expression construct was transfected along with IER5-HA (FL), IER5-49C-HA (lacking N-terminal 48 amino acids), and IER5-N156-HA (lacking C-terminal 171 amino acids) expression constructs. Cell extracts were subjected to immunoprecipitation analysis using an anti-HA antibody, and input (IN) and immunoprecipitated (IP) proteins were analyzed by western blotting. Positions of molecular mass markers are shown on the right.

(B) Co-immunoprecipitation analysis of B55 subunits with CDC25B. Myc-CDC25B* expression construct was transfected along with IER5-HA, B55α-HA, B55β-HA, B55γ-HA, and B55δ-HA expression constructs. Immunoprecipitation analysis was carried out using an anti-HA antibody as in (A).

(C, D) Phos-tag western blot analysis of CDC25B. Wild type HA-CDC25B* expression construct (C) and mutant HA-CDC25B* expression constructs (D) containing the indicated amino acid substitutions were transfected along with IER5-Myc expression construct. Cell extracts were subjected to SDS-PAGE with/without Phos-tag and analyzed by western blotting. Closed arrowheads and asterisk indicate discrete and faint smear bands separated by Phos-tag SDS-PAGE, respectively.

(E) Phosphorylation at Ser323 of CDC25B in IER5 expressing cells. Myc-CDC25B* expression construct was transfected along with IER5-HA derivative expression constructs. Okadaic acid (OA) was added to a final concentration of 150 nM for 1 h. Expression of IER5-HA derivatives was analyzed by western blotting using an anti-HA antibody. Myc-CDC25B* was immunoprecipitated by an anti-Myc antibody, and total and Ser323 phosphorylated Myc-CDC25B* were analyzed by western blotting using anti-Myc and anti-phospho-Ser323 antibodies. Numbers show the phosphorylated Ser323 levels determined after normalization to the Myc-CDC25B* levels.

(F) Stability of CDC25B-S323A in IER5 expressing cells. HA-CDC25B-S323A* and HA-GAPDH expression constructs were transfected along with IER5-HA expression construct. Cells were treated with 40 μg/ml cycloheximide (CHX) for 0, 30, and 60 min, and extracts were subjected to western blotting. Numbers show the HA-CDC25B-S323A* levels determined after normalization to the HA-GAPDH levels with comparison to the initial levels of control cells.

degradation was accelerated: the steady-state levels of HA-CDC25B* were 70% of control cells, and the half-life was 35 ± 5 min. These results suggest that IER5 negatively regulates the stability of CDC25B.

3.2. Dephosphorylation at serine 323 of CDC25B is involved in IER5-induced degradation

The interaction of CDC25B and IER5 was examined by co-immunoprecipitation analysis. When Myc-tagged CDC25B* expression construct was transfected along with HA-tagged IER5 expression construct, Myc-CDC25B* was co-immunoprecipitated with IER5-HA (FL) by an anti-HA antibody (Fig. 2A). A deletion derivative lacking the N-terminal IER homology region (IER5-49C-HA) was able to bind Myc-CDC25B*, whereas that lacking the C-terminal half of IER5 (IER5-N156-HA) failed to do so. IER5 interacts with PP2A via direct binding to the B55 family regulatory subunits [23]. Among four B55 members, α, β, γ, and δ, CDC25B preferentially bound to B55δ (Fig. 2B). Therefore, IER5 could assist the PP2A/B55δ-CDC25B interaction: its N-terminal region binds to PP2A/B55δ [21] and C-terminal half binds to CDC25B (see Fig. 2A).

On gels containing a phosphate-binding molecule Phos-tag, HA-CDC25B* was separated into ~5 bands, although it was identified as a single band on gels without Phos-tag (Fig. 2C). Co-transfection of IER5-Myc caused a decrease in slower migrating bands and an increase in faster migrating bands, showing that hypophosphorylated forms of CDC25B are predominant in IER5-Myc expressing cells. To explore which residues are involved in the phosphorylation, known phosphorylatable serine residues were substituted with alanine. A substitution at Ser323 (S323A) resulted in the disappearance of hyperphosphorylated bands of HA-CDC25B*, but other substitutions (S151A, S230A, S353A, or S375A) did not markedly affect the levels of phosphorylation. Notably, co-expression of IER5-Myc caused only slight changes in the phosphorylation status of HA-CDC25B-S323A*. In addition, the levels of HA-CDC25B-S323A* were slightly higher than those of the other

substitution mutants and were not substantially reduced by IER5-Myc. Western blot analysis using a phopsho-Ser323 antibody showed a decrease in the phosphorylation levels at Ser323 in IER5-HA (FL) expressing cells (Fig. 2E). The IER5-induced hypophosphorylation was not observed when the N-terminal (IER5-49C-HA) or C-terminal (IER5-N156-HA) region was deleted. The phosphorylation levels at Ser323 were rather increased by treatment of cells with the PP2A inhibitor okadaic acid (slower mobility of Myc-CDC25B* would be due to hyperphosphorylation). The deletion of either the N-terminal PP2A-interacting domain [21] or C-terminal CDC25B-binding region (see Fig. 2A) resulted in a loss of IER5 function, suggesting that IER5 assists the interaction of PP2A and CDC25B and enhances PP2A activity toward phosphorylated Ser323. As shown in Fig. 2F, the degradation rate of HA-CDC25B-S323A* was not accelerated by the expression of IER5-HA under steady-state conditions or in cycloheximide-treated cells. Therefore, IER5-induced dephosphorylation at Ser323 leads to degradation of CDC25B.

3.3. IER5 inhibits CDC25B binding to 14-3-3 but induces its binding to CDK1

It has been shown that phosphorylation at Ser323 mediates the interaction with 14-3-3 protein [9,10,14]. The immunoprecipitation analysis showed co-precipitation of HA-CDC25B* with 14-3-3β-Myc or 14-3-3ε-Myc by an anti-Myc antibody (Fig. 3A). The binding specificity was confirmed by the observation that 14-3-3ε-Myc containing amino acid substitutions in the phosphorylation-binding pocket (εM) failed to precipitate HA-CDC25B*. The S323A substitution disrupted the binding of CDC25B to 14-3-3β or 14-3-3ε. When IER5 was co-expressed, the binding of HA-CDC25B* to 14-3-3β-Myc was inhibited by full length IER5, whereas the N-terminal or C-terminal deletion derivatives, which fail to enhance dephosphorylation at Ser323, had no effect on the binding (Fig. 3B). The CDC25B binding to 14-3-3ε was also inhibited by IER5; however, addition of okadaic acid alleviated the inhibitory effect of IER5 (Fig. 3C). These results show that IER5-induced dephosphorylation at Ser323 leads to loss of the interaction between CDC25B and 14-3-3.

When a phosphatase-defective mutant of CDC25B (CDC25B**) was expressed in cells, Tyr15-phosphorylated CDK1 was co-immunoprecipitated with HA-CDC25B** by an anti-HA antibody (Fig. 3D). Expression of IER5 led to a slight increase in the levels of precipitated CDK1. It should be noted that 14-3-3 inhibits the binding of CDC25B to CDK1 [9,13], thus the S323A substitution enhanced co-precipitation of CDK1. Therefore, IER5 induces the binding of CDC25B to Tyr15-phosphorylated CDK1 through removal of 14-3-3.

3.4. 14-3-3 stabilizes CDC25B

To explore whether 14-3-3 affects the stability of CDC25B, the CDC25B levels in 14-3-3 overexpressing cells were analyzed by western blotting. As shown in Fig. 4A, overexpression of 14-3-3ε-Myc, but not its binding defective mutant, led to an increase in the steady-state levels of CDC25B. The levels of exogenously expressed Myc-CDC25B* were elevated by co-expression of increasing amounts of 14-3-3ε-Myc; however, those of HA-CDC25B* containing S323A substitution remained unaffected (Fig. 4B). The ubiquitin-proteasome system is the major pathway for the degradation of CDC25B [30–32]. Ubiquitination of CDC25B was analyzed by using cells expressing Myc-tagged ubiquitin. The anti-Myc western blot analysis of immunoprecipitated HA-CDC25B* showed the presence of high molecular weight smear bands of poly-ubiquitinated HA-CDC25B* (Fig. 4C). The levels of poly-ubiquitination were notably reduced by co-expression of 14-3-3ε-FLAG. This 14-3-3ε-dependent reduction was not observed when CDC25B contained the S323A substitution. These results show that 14-3-3 prevents ubiquitination of CDC25B thus stabilizes CDC25B via binding to phosphorylated Ser323.

3.5. 14-3-3 stabilizes CDC25A and inhibits CDC25A binding to CDK2

We next examined the effects of 14-3-3 on the stability and activity

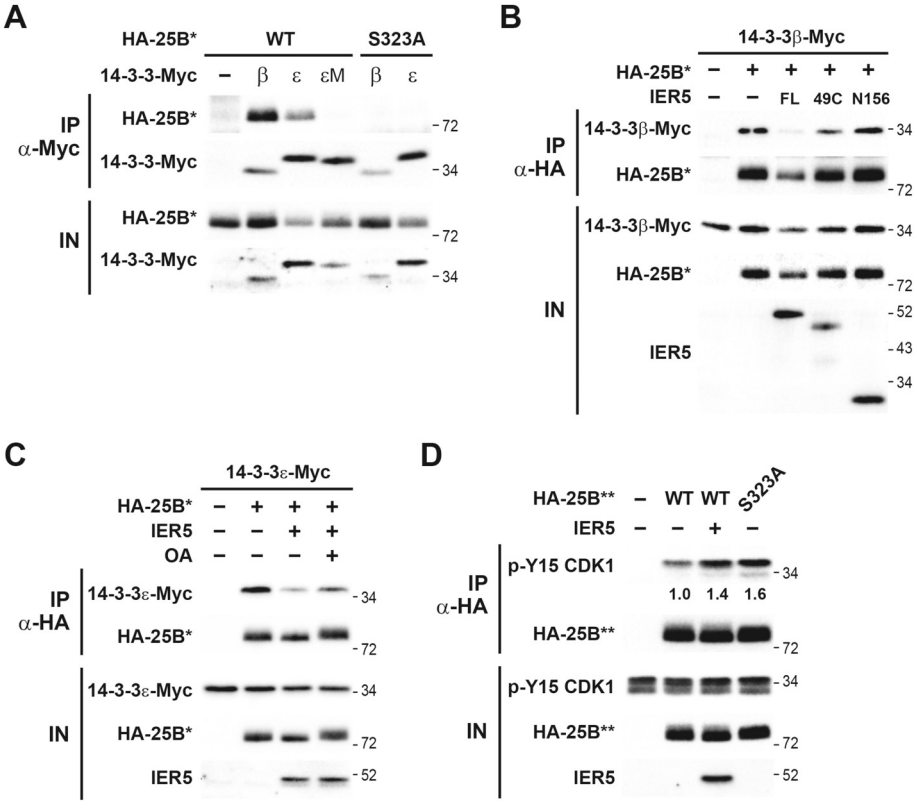

Fig. 3. Effects of IER5 on interaction between CDC25B and 14-3-3.
(A) Co-immunoprecipitation analysis of 14-3-3 with CDC25B. HA-CDC25B* (WT) and HA-CDC25B-S323A* expression constructs were transfected along with 14-3-3β-Myc, 14-3-3ε-Myc, and mutant 14-3-3ε-Myc (εM) expression constructs. Cell extracts were subjected to immunoprecipitation analysis using an anti-Myc antibody, and input (IN) and immunoprecipitated (IP) proteins were analyzed by western blotting. Positions of molecular mass markers are shown on the right.
(B) Interactions of 14-3-3β and CDC25B in IER5 expressing cells. HA-CDC25B* and 14-3-3β-Myc expression constructs were transfected along with IER5 derivative expression constructs. Immunoprecipitation analysis was carried out using an anti-HA antibody as in (A).
(C) Interactions of 14-3-3ε and CDC25B in IER5 expressing cells. HA-CDC25B* and 14-3-3ε-Myc expression constructs were transfected along with IER5 expression construct. Okadaic acid (OA) was added to a final concentration of 150 nM for 1 h. Immunoprecipitation analysis was carried out using an anti-HA antibody as in (A).
(D) Co-immunoprecipitation analysis of CDC25B with Tyr15-phosphorylated CDK1. HA-CDC25B** (WT) and HA-CDC25B-S323A** expression constructs were transfected along with IER5 expression construct. Immunoprecipitation analysis was carried out using an anti-HA antibody as in (A). Numbers show the precipitated CDK1 levels determined after normalization to the precipitated HA-CDC25B** levels.

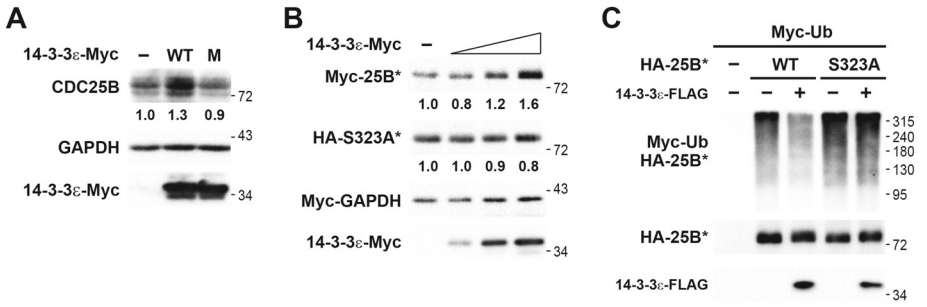

Fig. 4. Effects of 14-3-3ε on stability of CDC25B.
(A) CDC25B protein levels in 14-3-3ε overexpressing cells. Cells were transfected with wild type (WT) and mutant (M) 14-3-3ε-Myc expression constructs. Cell extracts were subjected to western blotting. Positions of molecular mass markers are shown on the right. Numbers show the relative CDC25B levels determined after normalization to the GAPDH levels.
(B) Levels of CDC25B and CDC25B-S323A in cells overexpressing 14-3-3ε. Myc-CDC25B*, HA-CDC25B-S323A*, and Myc-GAPDH expression constructs were transfected along with increasing amounts of 14-3-3ε-Myc expression constructs. Cell extracts were subjected to western blotting. Numbers show the Myc-CDC25B* and HA-CDC25B-S323A* levels determined after normalization to the Myc-GAPDH levels with comparison to the control levels.
(C) Ubiquitination of CDC25B. HA-CDC25B* (WT), HA-CDC25B-S323A*, and Myc-ubiquitin expression constructs were transfected along with 14-3-3ε-FLAG expression construct. Cells were treated with 20 μM MG132 for 1 h. Expression of 14-3-3ε-FLAG was analyzed by western blotting using an anti-FLAG antibody. Cell extracts were subjected to immunoprecipitation using an anti-HA antibody, and Myc-ubiquitin conjugated HA-CDC25B* and total HA-CDC25B* were analyzed by western blotting using anti-Myc and anti-HA antibodies.

of CDC25A. The immunoprecipitation analysis showed co-precipitation of 14-3-3ε-Myc with HA-CDC25A* (CDC25A* contained mutations in the CDK/Cyclin-docking site) (Fig. 5A). When cells were treated with okadaic acid, the levels of co-precipitated 14-3-3ε-Myc increased (slower mobility of HA-CDC25A* would be due to hyperphosphorylation). Phosphorylation at Ser178 and Thr507 of CDC25A is known to be necessary for the binding of 14-3-3 [12]. Treatment of cells with okadaic acid caused an increase in the phosphorylation levels at Ser178 and Thr507 (Fig. 5B). These results suggest that PP2A inhibits the interaction of CDC25A and 14-3-3ε via dephosphorylation at the 14-3-3-binding sites. The steady-state levels of Myc-CDC25A* were increased by 14-3-3ε-Myc overexpression but not by 14-3-3ε-Myc mutant defective for binding to phosphorylated amino acids (Fig. 5C). The increase was not observed when CDC25A* contained alanine substitutions at Ser178 and Thr507 (ST/AA). The binding of Thr14-phosphorylated CDK2 to CDC25A was observed when phosphatase defective mutant of HA-CDC25A (HA-CDC25A**) was immunoprecipitated by an anti-HA antibody (Fig. 5D). The ST/AA substitution further enhanced the binding of HA-CDC25A** to CDK2. Therefore, 14-3-3 regulates CDC25A similarly as CDC25B: its binding stabilizes CDC25A and inhibits the CDC25A-CDK2 interaction.

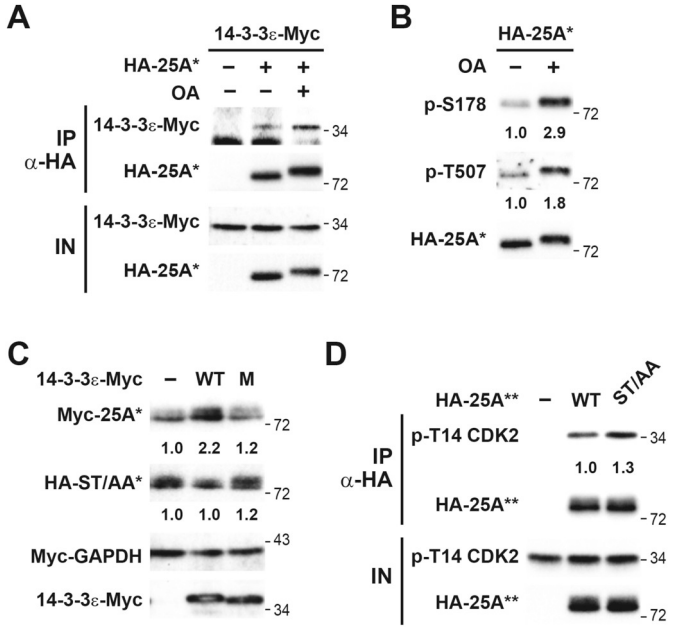

Fig. 5. Effects of 14-3-3ε on stability and activity of CDC25A.
(A) Co-immunoprecipitation analysis of 14-3-3ε with CDC25A. 14-3-3ε-Myc expression construct was transfected along with HA-CDC25A* expression construct. Okadaic acid (OA) was added to a final concentration of 150 nM for 1 h. Cell extracts were subjected to immunoprecipitation analysis using an anti-HA antibody, and input (IN) and immunoprecipitated (IP) proteins were analyzed by western blotting. Positions of molecular mass markers are shown on the right.
(B) Phosphorylation at Ser178 and Thr507 of CDC25A. Cells transfected with HA-CDC25A* expression construct were treated with 150 nM okadaic acid for 1 h. HA-CDC25A* was immunoprecipitated by an anti-HA antibody, and total, Ser178-phosphorylated, and Thr507-phosphorylated HA-CDC25A* were analyzed by western blotting using anti-HA, anti-phospho-Ser178, and anti-phospho-Thr507 antibodies. Numbers show the phosphorylated Ser178 and Thr507 levels determined after normalization to the HA-CDC25A* levels.
(C) Levels of CDC25A and CDC25A-ST/AA in cells overexpressing 14-3-3ε. Myc-CDC25A*, HA-CDC25A-ST/AA*, and Myc-GAPDH expression constructs were transfected along with wild type (WT) and mutant (M) 14-3-3ε-Myc expression constructs. Cell extracts were subjected to western blotting. Numbers show the Myc-CDC25A* and HA-CDC25A-ST/AA* levels determined after normalization to the Myc-GAPDH levels with comparison to the control levels.
(D) Co-immunoprecipitation analysis of CDC25A with Thr14-phosphorylated CDK2. Cells were transfected with HA-CDC25A** (WT) and HA-CDC25A-ST/AA** expression constructs. Immunoprecipitation analysis was carried out using an anti-HA antibody. Numbers show the precipitated CDK2 levels determined after normalization to the precipitated HA-CDC25A** levels.

3.6. Activity of CDC25A and CDC25B in heat-shocked cells

Elevated temperatures impede cell proliferation and induce G1/S and G2/M arrest [33]. When cells were exposed to heat shock at 42.5 °C for 40 min, the CDC25A levels were transiently decreased then increased up to 4 h of 37 °C recovery after heat exposure (Fig. 6A). Consistent with this, phosphorylation at Thr14 of CDK2 was maintained at low levels (Fig. 6B). When Thr14-phosphorylated CDK2 was co-immunoprecipitated with HA-CDC25A**, the levels of precipitated CDK2 in heat-shocked cells were slightly higher than those in control cells (Fig. 6C). In contrast, the levels of HA-CDC25A*-bound 14-3-3ε-Myc in heat-shocked cells were lower than those in control cells (Fig. 6D). Therefore, CDC25A dissociated from 14-3-3 becomes active, binds to CDK2, and dephosphorylates Thr14. As shown in Fig. 6A, the CDC25B levels sharply declined and remained low for at least 4 h of 37 °C recovery. The phosphorylation levels at Tyr15 of CDK1 were gradually increased in cells recovering from heat stress (Fig. 6E). Similarly to CDC25A, HA-CDC25B binding to phosphorylated CDK1 increased, whereas its binding to 14-3-3ε-Myc decreased in heat shocked cells compared to unheated cells (Fig. 6F and G). Although CDC25B would be active, the reduced CDC25B levels caused Tyr15 phosphorylation and inactivation of CDK1, leading to cell cycle arrest of heat-shocked cells.

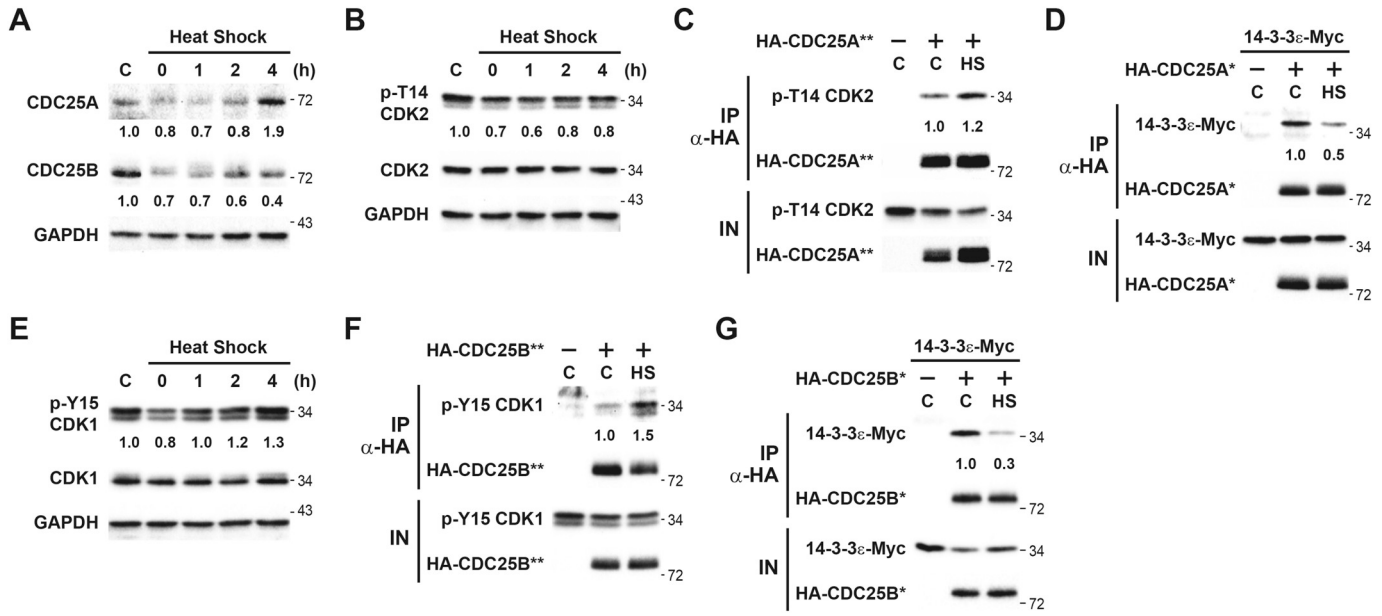

Fig. 6. CDC25A activity in heat-shocked cells.

(A) Levels of CDC25A and CDC25B. Cells cultured at 37 °C (C) were exposed to 42.5 °C for 40 min and allowed to recover at 37 °C for 0, 1, 2, and 4 h, and extracts were subjected to western blotting. Positions of molecular mass markers are shown on the right. Numbers show the relative CDC25A and CDC25B levels determined after normalization to the GAPDH levels.

(B) Levels of Thr14-phosphorylated CDK2. Cells were cultured as in (A). Numbers show the phosphorylated Thr14 levels determined after normalization to the total CDK2 levels.

(C) Interactions of CDC25A and Thr14-phosphorylated CDK2. Cells transfected with HA-CDC25A** expression construct were cultured at 37 °C (C), heat shocked at 42.5 °C 40 min, and allowed to recover at 37 °C for 1 h (HS). Cell extracts were subjected to immunoprecipitation analysis using an anti-HA antibody, and input (IN) and immunoprecipitated (IP) proteins were analyzed by western blotting. Numbers show the precipitated CDK2 levels determined after normalization to the precipitated HA-CDC25A** levels.

(D) Interactions of CDC25A and 14-3-3. Cells transfected with HA-CDC25A* and 14-3-3ε-Myc expression constructs were cultured as in (C). Immunoprecipitation analysis was carried out using an anti-HA antibody. Numbers show the precipitated 14-3-3ε-Myc levels determined after normalization to the precipitated HA-CDC25A* levels.

(E) Levels of Tyr15-phosphorylated CDK1. Cells were cultured as in (A). Numbers show the phosphorylated Tyr15 levels determined after normalization to the total CDK1 levels.

(F) Interactions of CDC25B and Tyr15-phosphorylated CDK1. Cells transfected with HA-CDC25B** expression construct were cultured as in (C). Immunoprecipitation analysis was carried out using an anti-HA antibody. Numbers show the precipitated CDK1 levels determined after normalization to the precipitated HA-CDC25B** levels.

(G) Interactions of CDC25B and 14-3-3. Cells transfected with HA-CDC25B* and 14-3-3ε-Myc expression constructs were cultured as in (C). Immunoprecipitation analysis was carried out using an anti-HA antibody. Numbers show the precipitated 14-3-3ε-Myc levels determined after normalization to the precipitated HA-CDC25B* levels.

4. Discussion

CDC25A and CDC25B are very unstable proteins, and their levels are tightly regulated during cell cycle. The PP2A B55δ subunit and PP2A regulatory protein IER5 bind to CDC25B. IER5 induces PP2A phosphatase activity toward Ser323 of CDC25B, which results in the dissociation of 14-3-3 proteins from CDC25B. 14-3-3 proteins inhibit CDC25B ubiquitination and CDC25B binding to CDK1, suggesting that PP2A/IER5 enhances turnover of CDC25B. The 14-3-3 binding also causes stabilization of CDC25A and inhibition of the CDC25A-CDK2 interaction. In heat-shocked cells, CDC25A and CDC25B dissociate from 14-3-3 and bind to phophorylated CDKs. Therefore, the 14-3-3 interaction regulates the stability and activity of both CDC25A and CDC25B.

Previous report has shown that IER5 represses transcription of the *CDC25B* gene [17]. Here, we have demonstrated that IER5 induces degradation of CDC25B. IER5 binds to both the PP2A B55 subunit and PP2A target proteins and regulates the substrate specificity of PP2A [21–23]. Consistently, IER5 derivatives lacking the N-terminal B55-interacting domain or C-terminal CDC25B-binding region fail to enhance hypophosphorylation at Ser323 of CDC25B. Under normal physiological and various stressed conditions, Ser323 is targeted by many kinases, including CHK1, PKA, pEg3, p38, and p38-activted protein kinase 2 (MK2) [34–40]. The phosphorylation is maintained during S to G2 and reduced in mitosis [14,34]. During interphase, phospho-Ser323-dependent binding of CDC25B to 14-3-3 stabilizes CDC25B, blocks CDC25B activity toward CDK1, and sequesters CDC25B in the cytoplasm. IER5 expression is upregulated by treatment of cells with ionizing radiation and anti-cancer agents, and increased IER5 potentiates G2/M cell cycle arrest [17,20]. In contrast, decreased IER5 and low PP2A activity associate with an increase in CDC25B expression [17,18,41], and overexpression of CDC25B overrides radiation-induced G2/M arrest [42]. Therefore, IER5 assists PP2A-mediated dephosphorylation at Ser323, which leads to the dissociation of CDC25B from 14-3-3, CDC25B degradation, and G2/M arrest.

5. Conclusions

In assistance with IER5, PP2A converts CDC25B to an unstable, but slightly active, form through removal of 14-3-3. The PP2A/IER5-CDC25B signaling pathway would be important in the G2-M transition. The stability and activity of CDC25A is also regulated by 14-3-3, suggesting that the control of the 14-3-3 binding is a major mechanism regulating CDC25A and CDC25B functions.

Acknowledgements

This work was supported in part by JSPS KAKENHI (grant no. 16K07292).

Conflict of interest

The authors declare no conflict of interest.

Author contributions

Y.K., M.S., and M.Y. performed experiments and analyzed the data; H.S. planned the experiments and wrote the paper.

References

[1] R. Boutros, V. Lobjois, B. Ducommun, CDC25 phosphatases in cancer cells: key players? Good targets? Nat. Rev. Cancer 7 (7) (2007) 495–507, https://doi.org/10.1038/nrc2169.

[2] S. Sur, D.K. Agrawal, Phosphatases and kinases regulating CDC25 activity in the cell cycle: clinical implications of CDC25 overexpression and potential treatment strategies, Mol. Cell. Biochem. 416 (1–2) (2016) 33–46, https://doi.org/10.1007/s11010-016-2693-2.

[3] N. Hégarat, S. Rata, H. Hochegger, Bistability of mitotic entry and exit switches during open mitosis in mammalian cells, BioEssays 38 (7) (2016) 627–643, https://doi.org/10.1002/bies.201600057.

[4] H.C. Reinhardt, M.B. Yaffe, Kinases that control the cell cycle in response to DNA damage: Chk1, Chk2, and MK2, Curr. Opin. Cell Biol. 21 (2) (2009) 245–255, https://doi.org/10.1016/j.ceb.2009.01.018.

[5] H.C. Reinhardt, M.B. Yaffe, Phospho-Ser/Thr-binding domains: navigating the cell cycle and DNA damage response, Nat. Rev. Mol. Cell Biol. 14 (9) (2013) 563–580, https://doi.org/10.1038/nrm3640.

[6] N.N. Sluchanko, N.B. Gusev, Moonlighting chaperone-like activity of the universal regulatory 14-3-3 proteins, FEBS J. 284 (9) (2017) 1279–1295, https://doi.org/10.1111/febs.13986.

[7] K.L. Pennington, T.Y. Chan, M.P. Torres, J.L. Andersen, The dynamic and stress-adaptive signaling hub of 14-3-3: emerging mechanisms of regulation and context-dependent protein-protein interactions, Oncogene 37 (42) (2018) 5587–5604, https://doi.org/10.1038/s41388-018-0348-3.

[8] N. Davezac, V. Baldin, B. Gabrielli, A. Forrest, N. Theis-Febvre, M. Yashida, B. Ducommun, Regulation of CDC25B phosphatases subcellular localization, Oncogene 19 (18) (2000) 2179–2185, https://doi.org/10.1038/sj.onc.1203545.

[9] N. Giles, A. Forrest, B. Gabrielli, 14-3-3 acts as an intramolecular bridge to regulate cdc25B localization and activity, J. Biol. Chem. 278 (31) (2003) 28580–28587, https://doi.org/10.1074/jbc.M304027200.

[10] S. Uchida, A. Kuma, M. Ohtsubo, M. Shimura, M. Hirata, H. Nakagama, T. Matsunaga, Y. Ishizaka, K. Yamashita, Binding of 14-3-3β but not 14-3-3σ controls the cytoplasmic localization of CDC25B: binding site preferences of 14-3-3 subtypes and the subcellular localization of CDC25B, J. Cell Sci. 117 (2004) 3011–3020, https://doi.org/10.1242/jcs.01086 Pt 14.

[11] S.N. Dalal, C.M. Schweitzer, J. Gan, J.A. Decaprio, Cytoplasmic localization of human cdc25C during interphase requires an intact 14-3-3 binding site, Mol. Cell. Biol. 19 (6) (1999) 4465–4479, https://doi.org/10.1128/MCB.19.6.4465.

[12] M.S. Chen, C.E. Ryan, H. Piwnica-Worms, Chk1 kinase negatively regulates mitotic function of Cdc25A phosphatase through 14-3-3 binding, Mol. Cell. Biol. 23 (21) (2003) 7488–7497, https://doi.org/10.1128/MCB.23.21.7488-7497.2003.

[13] A. Forrest, B. Gabrielli, Cdc25B activity is regulated by 14-3-3, Oncogene 20 (32) (2001) 4393–4401, https://doi.org/10.1038/sj.onc.1204574.

[14] P. Astuti, R. Boutros, B. Ducommun, B. Gabrielli, Mitotic phosphorylation of Cdc25B Ser321 disrupts 14-3-3 binding to the high affinity Ser323 site, J. Biol. Chem. 285 (45) (2010) 34364–34370, https://doi.org/10.1074/jbc.M110.138412.

[15] P. Astuti, B. Gabrielli, Phosphorylation of Cdc25B3 Ser169 regulates 14-3-3 binding to Ser151 and Cdc25B activity, Cell Cycle 10 (12) (2011) 1960–1967, https://doi.org/10.4161/cc.10.12.15819.

[16] K. Kasahara, H. Goto, M. Enomoto, Y. Tomono, T. Kiyono, M. Inagaki, 14-3-3γ mediates Cdc25A proteolysis to block premature mitotic entry after DNA damage, EMBO J. 29 (16) (2010) 2802–2812, https://doi.org/10.1038/emboj.2010.157.

[17] S. Nakamura, Y. Nagata, L. Tan, T. Takemura, K. Shibata, M. Fujie, S. Fujisawa, Y. Tanaka, M. Toda, R. Makita, K. Tsunekawa, M. Yamada, M. Yamaoka, J. Yamashita, K. Ohnishi, M. Yamashita, Transcriptional repression of Cdc25B by IER5 inhibits the proliferation of leukemic progenitor cells through NF-YB and p300 in acute myeloid leukemia, PLoS One 6 (11) (2011) e28011, https://doi.org/10.1371/journal.pone.0028011.

[18] C. Pan, D. Zhu, Y. Wang, L. Li, D. Li, F. Liu, C.Y. Zhang, K. Zen, Human cytomegalovirus miR-UL148D facilitates latent viral infection by targeting host cell immediate early response gene 5, PLoS Pathog. 12 (11) (2016) e1006007, https://doi.org/10.1371/journal.ppat.1006007.

[19] K.K. Ding, Z.F. Shang, C. Hao, Q.Z. Xu, J.J. Shen, C.J. Yang, Y.H. Xie, C. Qiao, Y. Wang, L.L. Xu, P.K. Zhou, Induced expression of the IER5 gene by gamma-ray irradiation and its involvement in cell cycle checkpoint control and survival, Radiat. Environ. Biophys. 48 (2) (2009) 205–213, https://doi.org/10.1007/s00411-009-0213-4.

[20] C. Yang, Y. Wang, C. Hao, Z. Yuan, X. Liu, F. Yang, H. Jiang, X. Jiang, P. Zhou, K. Ding, IER5 promotes irradiation- and cisplatin-induced apoptosis in human hepatocellular carcinoma cells, Am. J. Transl. Res. 8 (4) (2016) 1789–1798.

[21] S. Kawabata, Y. Ishita, Y. Ishikawa, H. Sakurai, Immediate-early response 5 (IER5) interacts with protein phosphatase 2A and regulates the phosphorylation of ribosomal protein S6 kinase and heat shock factor 1, FEBS Lett. 589 (23) (2015) 3679–3685, https://doi.org/10.1016/j.febslet.2015.10.013.

[22] Y. Asano, T. Kawase, A. Okabe, S. Tsutsumi, H. Ichikawa, S. Tatebe, I. Kitabayashi, F. Tashiro, H. Namiki, T. Kondo, K. Semba, H. Aburatani, Y. Taya, H. Nakagama, R. Ohki, IER5 generates a novel hypo-phosphorylated active form of HSF1 and contributes to tumorigenesis, Sci. Rep. 6 (2016) 19174, https://doi.org/10.1038/srep19174.

[23] Y. Ishikawa, S. Kawabata, H. Sakurai, HSF1 transcriptional activity is modulated by IER5 and PP2A/B55, FEBS Lett. 589 (10) (2015) 1150–1155, https://doi.org/10.1016/j.febslet.2015.03.019.

[24] N. Wlodarchak, Y. Xing, PP2A as a master regulator of the cell cycle, Crit. Rev. Biochem. Mol. Biol. 51 (3) (2016) 162–184, https://doi.org/10.3109/10409238.2016.1143913.

[25] J. Sangodkar, C.C. Farrington, K. McClinch, M.D. Galsky, D.B. Kastrinsky, G. Narla, All roads lead to PP2A: exploiting the therapeutic potential of this phosphatase, FEBS J. 283 (6) (2016) 1004–1024, https://doi.org/10.1111/febs.13573.

[26] S.T. Chou, Y.C. Yen, C.M. Lee, M.S. Chen, Pro-apoptotic role of Cdc25A: activation of cyclin B1/Cdc2 by the Cdc25A C-terminal domain, J. Biol. Chem. 285 (23) (2010) 17833–17845, https://doi.org/10.1074/jbc.M109.078386.

[27] X. Xu, S.P. Burke, Roles of active site residues and the NH_2-terminal domain in the catalysis and substrate binding of human Cdc25, J. Biol. Chem. 271 (9) (1996) 5118–5124, https://doi.org/10.1074/jbc.271.9.5118.

[28] M.B. Yaffe, K. Rittinger, S. Volinia, P.R. Caron, A. Aitken, H. Leffers, S.J. Gamblin, S.J. Smerdon, L.C. Cantley, The structural basis for 14-3-3: phosphopeptide binding specificity, Cell 91 (7) (1997) 961–971, https://doi.org/10.1016/S0092-8674(00)80487-0.

[29] M. Nagashimada, T. Ueda, Y. Ishita, H. Sakurai, TAF7 is a heat-inducible unstable protein and is required for sustained expression of heat shock protein genes, FEBS J. 285 (17) (2018) 3215–3224, https://doi.org/10.1111/febs.14604.

[30] V. Baldin, C. Cans, M. Knibiehler, B. Ducommun, Phosphorylation of human CDC25B phosphatase by CDK1-cyclin a triggers its proteasome-dependent degradation, J. Biol. Chem. 272 (52) (1997) 32731–32734, https://doi.org/10.1074/jbc.272.52.32731.

[31] Y. Kanemori, K. Uto, N. Sagata, β-TrCP recognizes a previously undescribed non-phosphorylated destruction motif in Cdc25A and Cdc25B phosphatases, Proc. Natl. Acad. Sci. U. S. A. 102 (18) (2005) 6279–6284, https://doi.org/10.1073/pnas.0501873102.

[32] S. Uchida, N. Watanabe, Y. Kudo, K. Yoshioka, T. Matsunaga, Y. Ishizaka, H. Nakagama, R.Y. Poon, K. Yamashita, $SCF^{\beta TrCP}$ mediates stress-activated MAPK-induced Cdc25B degradation, J. Cell Sci. 124 (2011) 2816–2825, https://doi.org/10.1242/jcs.083931 Pt 16.

[33] A.K. Velichko, E.N. Markova, N.V. Petrova, S.V. Razin, O.L. Kantidze, Mechanisms of heat shock response in mammals, Cell. Mol. Life Sci. 70 (22) (2013) 4229–4241, https://doi.org/10.1007/s00018-013-1348-7.

[34] D.V. Bulavin, Y. Higashimoto, I.J. Popoff, W.A. Gaarde, V. Basrur, O. Potapova, E. Appella, A.J. Fornace Jr., Initiation of a G2/M checkpoint after ultraviolet radiation requires p38 kinase, Nature 411 (6833) (2001) 102–107, https://doi.org/10.1038/35075107.

[35] N. Davezac, V. Baldin, J. Blot, B. Ducommun, J.P. Tassan, Human pEg3 kinase associates with and phosphorylates CDC25B phosphatase: a potential role for pEg3 in cell cycle regulation, Oncogene 21 (50) (2002) 7630–7641, https://doi.org/10.1038/sj.onc.1205870.

[36] I.A. Manke, A. Nguyen, D. Lim, M.Q. Stewart, A.E. Elia, M.B. Yaffe, MAPKAP kinase-2 is a cell cycle checkpoint kinase that regulates the G2/M transition and S phase progression in response to UV irradiation, Mol. Cell 17 (1) (2005) 37–48, https://doi.org/10.1016/j.molcel.2004.11.021.

[37] M. Lemaire, C. Froment, R. Boutros, O. Mondesert, A.R. Nebreda, B. Monsarrat, B. Ducommun, CDC25B phosphorylation by p38 and MK-2, Cell Cycle 5 (15) (2006) 1649–1653, https://doi.org/10.4161/cc.5.15.3006.

[38] H. Cha, X. Wang, H. Li, A.J. Fornace Jr., A functional role for p38 MAPK in modulating mitotic transit in the absence of stress, J. Biol. Chem. 282 (31) (2007) 22984–22992, https://doi.org/10.1074/jbc.M700735200.

[39] J.P. Bouché, C. Froment, C. Dozier, C. Esmenjaud-Mailhat, M. Lemaire, B. Monsarrat, O. Burlet-Schiltz, B. Ducommun, NanoLC-MS/MS analysis provides new insights into the phosphorylation pattern of Cdc25B in vivo: full overlap with sites of phosphorylation by Chk1 and Cdk1/cycB kinases in vitro, J. Proteome Res. 7 (3) (2008) 1264–1273, https://doi.org/10.1021/pr700623p.

[40] Y. Zhang, Z. Zhang, X.Y. Xu, X.S. Li, M. Yu, A.M. Yu, Z.H. Zong, B.Z. Yu, Protein kinase a modulates Cdc25B activity during meiotic resumption of mouse oocytes, Dev. Dyn. 237 (12) (2008) 3777–3786, https://doi.org/10.1002/dvdy.21799.

[41] C.I. Ko, Y. Fan, M. de Gannes, Q. Wang, Y. Xia, A. Puga, Repression of the aryl hydrocarbon receptor is required to maintain mitotic progression and prevent loss of pluripotency of embryonic stem cells, Stem Cells 34 (12) (2016) 2825–2839, https://doi.org/10.1002/stem.2456.

[42] H. Miyata, Y. Doki, H. Yamamoto, K. Kishi, H. Takemoto, Y. Fujiwara, T. Yasuda, M. Yano, M. Inoue, H. Shiozaki, I.B. Weinstein, M. Monden, Overexpression of CDC25B overrides radiation-induced G2-M arrest and results in increased apoptosis in esophageal cancer cells, Cancer Res. 61 (7) (2001) 3188–3193.